NRL Memorandum Report 3953

Application of Coatings by High Energy CW Lasers

R. J. SCHAEFER, J. D. AYERS, AND T. R. TUCKER

Alloy Transformations & Kinetics Branch
Material Science and Technology Division

LEVEL II

March 30, 1979

NAVAL RESEARCH LABORATORY
Washington, D.C.

SECURITY CLASSIFICATION OF THIS PAGE (When Data Entered)

REPORT DOCUMENTATION PAGE

READ INSTRUCTIONS BEFORE COMPLETING FORM

1. REPORT NUMBER: NRL Memorandum Report 3953	2. GOVT ACCESSION NO.
3. RECIPIENT'S CATALOG NUMBER	
4. TITLE (and Subtitle): APPLICATION OF COATINGS BY HIGH ENERGY CW LASERS	5. TYPE OF REPORT & PERIOD COVERED: Semi-annual 1 Apr. 78 – 1 Oct. 78
6. PERFORMING ORG. REPORT NUMBER	
7. AUTHOR(s): R. J. Schaefer, J. D. Ayers, and T. R. Tucker	8. CONTRACT OR GRANT NUMBER(s): ARPA Order No. 3579
9. PERFORMING ORGANIZATION NAME AND ADDRESS: Naval Research Laboratory, Washington, D.C. 20375	10. PROGRAM ELEMENT, PROJECT, TASK AREA & WORK UNIT NUMBERS: 62712E, NRL Problem M01-73.501
11. CONTROLLING OFFICE NAME AND ADDRESS: Defense Advanced Research Projects Agency, 1400 Wilson Boulevard, Arlington, VA 22209 (Dr. M. Buckley)	12. REPORT DATE: March 30, 1979
	13. NUMBER OF PAGES: 35
14. MONITORING AGENCY NAME & ADDRESS (if different from Controlling Office)	15. SECURITY CLASS. (of this report): UNCLASSIFIED
	15a. DECLASSIFICATION/DOWNGRADING SCHEDULE

16. DISTRIBUTION STATEMENT (of this Report)

Approved for public release; distribution unlimited.

17. DISTRIBUTION STATEMENT (of the abstract entered in Block 20, if different from Report)

18. SUPPLEMENTARY NOTES

19. KEY WORDS (Continue on reverse side if necessary and identify by block number)

Laser
Coatings
Powder
Pyrometry

20. ABSTRACT (Continue on reverse side if necessary and identify by block number)

The objective of this program is to apply coatings to the surface of metals using the high energy density heating of CW lasers. The coatings are applied by either the laser spray process, in which powder is heated and propelled to the substrate surface for deposition, or by plasma spraying with subsequent laser remelt. This report describes the development of methods for carrying out and analyzing these processes, the selection of materials, and the early experimental results. The kinetics of laser spraying of aluminum oxide in air are reported.

DD FORM 1 JAN 73 1473 EDITION OF 1 NOV 65 IS OBSOLETE
S/N 0102-014-6601

SECURITY CLASSIFICATION OF THIS PAGE (When Data Entered)

CONTENTS

SECTION I
INTRODUCTION

The current intense research on materials produced by rapid solidification, combined with the availability of lasers which can be focused to give extremely high radiant power density, has generated much interest in the use of lasers for surface heat treatment of materials. Early experiments investigated the changes of surface microstructure which could be made without changes in the material composition. A much wider range of useful surface properties could be generated if alloying elements were added concurrent with the laser heat treatment.

Although numerous methods are presently available for the application of coatings, it is frequently found that no method is adequate for producing coatings for use in severe environments. Poor adhesion to the substrate and porosity or inhomogeneity of the coating are some of the most frequent problems. Because laser heating can be used to fuse the surface of materials without greatly heating their bulk, it can solve these coating problems without thermally degrading the substrate.

The objective of this program is to develop methods for applying protective coatings by the laser spray process and by the plasma spray plus laser remelt process. The microstructure and the protective properties of these coatings will be characterized. A particle pyrometry system has been developed to analyze the thermal behavior of hot particles moving rapidly in the laser beam.

The Laser Spraying Concept

It is well known that momentum is transfered to solids which are impacted by high energy pulsed laser beams: CW beams of sufficient power density also can impart momentum to solids. Although high levels of force or pressure may not be attained, significant accelerations may be imparted to small particles.

The process of photophoresis, in which light causes particles to move by preferentially heating the surrounding atmosphere on one side of a particle, and thus increasing the pressure on that side, has been analyzed by several authors (1, 2). With the radiation levels available from high-energy lasers, vaporization from the particle surface becomes an important driving mechanism. Particles may be heated to well above their melting points and achieve high downstream velocities in the laser beam. Radiation pressure,

Note: Manuscript submitted January 15, 1979.

due to photon momentum , can make an additional contribution to propulsion of the particles.

When these mechanisms of particle propulsion are combined with the concepts of laser surface heating, in which a laser beam of high energy density is used to rapidly heat a material surface with subsequent rapid cooling by heat flow to the interior of the material, we derive the concept of "laser spraying." In this process (Fig. 1), a coating is applied to a material by introducing a powder of the coating material into a laser beam. The beam heats the powder particles and propels them toward a substrate where they impinge to form a coating. By bringing the laser beam to a focus at or near the substrate surface, a thin layer may be melted on this surface to obtain maximum fusion of coating to substrate. In cases where mixing of coating and substrate materials is undesirable, the laser beam can be adjusted to avoid high maximum temperatures at the substrate surface.

The laser spraying process is well suited to the formation of corrosion resisting coatings because it results in rapid solidification of the coating material, with the result that this material can be microcrystalline or amorphous. Particles which attain extremely high temperatures in the laser beam are solidified as they impinge on the substrate surface. The first evidence of this rapid solidification was seen in aluminum oxide particles deposited on copper and aluminum substrates. Those particles which impinged with the highest velocities spread out and wet the surface, and these particles are glassy clear in appearance, indicating that they are either amorphous or have crystallite sizes well below the wavelength of light. Particles which did not wet so well cooled more slowly and had a cloudy or opaque appearance.

Many wear-resisting coatings contain extremely hard particles of carbides or Laves phases in a matrix of more ductile material. To produce such coatings by laser spraying, one can spray mixed powders (such as titanium carbide and a ductile ferrous composition). In such systems the laser beam parameters should be selected to result in limited fusion of the hard and ductile phases and of the substrate.

The Plasma-Spray Plus Remelt Concept

The second major line of research within this project is to explore the potential for improvement of properties which can result from laser remelting of plasma-sprayed

coatings. This concept is not new, for the first patent on the process dates back to 1963 (3). It is only in the last few years, with the accessability of multikilowatt CW lasers, that experimental work has proceeded. Even now there is very little published information available on experimental results, partly because the work is considered proprietary. Most of the information which is available comes from the Avco Everett Research Laboratory, and it deals largely with increasing the chromium content in the surface layer of steels. This program will survey the remelt characteristics of a series of commercial and experimental corrosion and wear preventing coatings.

Corrosion preventing coatings applied by the plasma spray process, for a wide range of application, degrade more rapidly than desired in service for three basic reasons: inappropriate chemistry, chemical inhomogeneity, and lack of structural integrity in the as deposited coating. Laser remelting cannot, of course, make any beneficial changes in the nominal coating chemistry, but with some coatings significant improvements can be made in chemical homogeneity and in structural integrity. Because solidification of thin laser melted surface layers is very rapid, partitioning of alloying elements is minimized, thus minimizing the chemical activity of localized galvanic corrosion cells. These cells can take the form of separate phases or of partitioning to grain boundaries - in either case rapid solidification is beneficial. Perhaps the ideal structure, with respect to chemical partitioning, is an amorphous phase. We hope to produce such a structure in the form of an amorphous coating on a steel substrate. Candidate materials, to be discussed later, have been prepared.

Structural integrity of plasma sprayed coatings can be improved both by fusing the coating to the substrate and by closing the pores which are nearly always present. For corrosion prevention these pores pose a special problem because the corrosion producing fluid can penetrate through the pores to the substrate. In the case of wear resisting coatings, improving adhesion to the substrate and closing the pores can both toughen the coating appreciably. Only when lubricant retention within the pores is desirable would eliminating them not prove beneficial.

Unlike most corrosion preventing coatings, it is often desirable for wear resistant coatings to consist of two phases with markedly different properties. The directional solidification aspect of laser melting can be exploited in this respect to produce microstructures with the hard, wear

resisting phase alligned in rod or plate-like forms normal to the substrate surface. Such structures will be studied because they should prove superior to randomly distributed ones.

SECTION II
POWDERS IN LASER BEAMS

Theory

The temperature history of powder particles in a CW infrared laser beam can be calculated assuming several physical idealizations. For incident beam power densities less than $10^5 W/cm^2$, plasma effects can be ignored leaving three principle energy transfer mechanisms. Particles are heated by direct absorption of the incoming radiation and liberate energy by thermal radiation. If an atmosphere is present, particles also lose energy to the gas by convection. In equilibrium, the absorbed energy must equal the energy loss; otherwise, the temperature change is proportional to the difference in these terms.

We make the following simplifying assumptions: the density of powder particles is considered low enough that collective effects (laser reflection, refraction, interparticle heating, beam shadowing) can be neglected. The particles are spherical with variable radius R. For these first calculations, the flux is uniform and constant. The particle temperature is assumed to be uniform. Rough calculations indicate that surface temperatures may vary as much as 20% from illuminated to dark side. It is not now clear how much calculational error is introduced by a temperature gradient of this magnitude.

$$F_{abs} = \pi R^2 \alpha J \qquad (1)$$

where α is the particle absorptivity at the laser wavelength. The particle radiant energy loss follows the Stefan-Boltzmann equation

$$F_{rad} = 4\pi R^2 \varepsilon\ (T) \sigma\ T^4 \qquad (2)$$

where ε is the total emissivity, σ is the Stefan-Boltzmann constant, and T is the absolute temperature in K.

For irradiation in air, certain assumptions must be made concerning particle motion. Measured particle velocities and sizes indicate relatively low Reynolds number flows. Thus, lamellar flow in the stagnation limit is assumed for the convection loss term.

$$H(T) \simeq \frac{1}{R} K_f \ (T/2) \qquad (3)$$

where H is the surface coefficient of heat transfer and K_f is the thermal conductivity of the surrounding medium at the film temperature (T/2). The energy loss becomes

$$F_{conv} = 4\pi R^2 H(T) = 4\pi R K_f (T/2) \qquad (4)$$

For a small time interval t, the temperature rise is as follows

$$\Delta T = \frac{3\Delta t}{4\pi\rho R^3 C(T)} \left[F_{abs} - F_{conv} - F_{rad}\right] \qquad (5)$$

where ρ is the particle material density and C is the specific heat. Since ΔT depends on both time and temperature, the temperature history must be calculated by finite difference.

The procedure above is applied to 40 μm alumina particles exposed to fluxes of 2-10 kW/cm^2 in Figure 2. The irradiation takes place in air. Log T is plotted versus log of interaction time. For J = $2kW/cm^2$, the melt temperature (2300°K) is not reached; for J = $4kW/cm^2$, the particle becomes a molten droplet; at 8 kW/cm^2, the illuminated surface should reach the boiling point; at $10kW/cm^2$, the code predicts total particle vaporization. Ultimate temperature is reached by 0.05 second.

Figure 3 shows the temperature profiles for 40μm Al_2O_3 particles in vacuum. Note the much higher maximum temperatures for a given flux than were attained during the atmospheric irradiations of Figure 2. The difference indicates the importance of convective cooling in the control of powder temperatures.

Similar calculations have been applied to previously conducted Al_2O_3 powder experiments using a converging 10.6μm laser beam in air. The result is shown in the photographic exposure of Figure 4. The laser beam is incident from the left and focusing toward the right. The powder injection nozzle can be seen on the extreme left. The lower horizontal axis marks the horizontal distance from the nozzle while the upper scale estimates the average laser flux at that location. Arrows note the fluxes where 50 and 25μm-radii particles are predicted to melt.

The particles first become visible in the photograph at the melting region and become much brighter thereafter. This behavior is consistent with other photographic tests which indicated that alumina particles below the melt point were practically invisible when heated by flames. Powders which were subsequently found to be melted, had sufficient luminoisity for detection. Therefore, the calculations appear to have general validity.

Initial Experiments

The initial verification of the laser spraying process was carried out using aluminum oxide powder. This material was chosen because it can be heated in air without degradation: it is also a good absorber of 10.6 μm radiation. The initial experiments were intended to demonstrate that propulsion took place, to measure the velocities of the powder particles,to determine if the particles suffered excessive material loss due to vaporization, and to demonstrate that the particles could be deposited on metallic substrates.

In the first experiments, powder was simply dropped from a small funnel into a horizontal laser beam. It was dramatically evident that some of the powder was heated to an extremely high temperature and propelled in the laser beam. Powder which was collected after downstream transport was found to have been transformed into spheres, indicating that it had been molten. However, convective air flow resulted in a very low efficiency of powder insertion into the laser beam, and some powder was transported by air currents and fell into the stream at points upstream or downstrem from the funnel. Better injection mechanisms were needed to allow quantitative studies of powder propulsion.

For a subsequent series of experiments, powder was inserted into the laser beam by means of both a water-cooled nozzle which was inserted into the center of the beam, and a mirror with a very small hole through which powder was blown into the reflected beam. These mechanisms resulted in a much higher powder insertion efficiency and virtual elimination of convection effects near the injection point. A more detailed description of these devices is found in Section IV.

The velocities of particles in the laser beam were determined photographically, using a light chopper arrangement (also described in Section IV).

It was found that the most effective heating of powder particles resulted when the powder was injected into the beam with the minmum velocity needed to suspend it in the transport gas, which was in the range of 0.5 to 1 m/sec.

Measured velocities of particles in a 6 kw laser beam which was rapidly converging toward a focus were found to be increasing with time, with the greatest velocities slightly above 4m/sec. Because the particles were moving into regions of progressively higher energy density, it was not possible to distinguish how much of this acceleration was due to the increasing power density and how much was due to an approach to a steady state velocity. Additional experiments, in which particle velocities are measured at different points in the beam, will clarify this point.

One concern, in view of the evaporative propulsion mechanism, was that excessive material would be lost from the powder particles. To investigate this effect, collectors were placed under the laser beam at various distances downstream from the injection nozzle, and closely size-sorted powder was injected into the beam. The size distribution of the collected powders, which had been melted and spheroidized, was then determined.

The results shown in Figure 5 from a test in a 6 kw beam, indicate at most a small decrease in particle diameter resulting from transport in the beam. It is concluded that evaporative loss is not a serious problem in this system.

SECTION III
SURFACE MELTING

Materials Selection and Preparation

A series of materials has been prepared for laser remelt processing. The materials include conventional hardfacing alloys, commercial coatings resistant to corrosion, experimental corrosion resistant coatings, and materials selected with the specific objective of obtaining amorphous surface layers on engineering alloys. Hardfacing alloys in bulk form which will be tested for response to laser remelting include Tribaloys 400, 700, and 800 (a series of cobalt based alloys in which a Co_2Mo Laves phase contributes to wear resistance) and Ferrotic C (a powder metallurgy product consisting of TiC in a ferrous matrix).

If the Tribaloys respond favorably to laser remelting they will be prepared as coatings on engineering materials

for further testing. The Ferrotic C has already been acquired as a plasma sprayed coating on a tool steel substrate, so a comparison can be made of its behavior in the two conditions. Additional wear resisting materials which have been prepared as plasma spray coatings are listed in Table I. These and other plasma sprayed materials were secured on contract from APS Materials in Dayton, Ohio. The materials of Table I were selected because they are representative of different types of wear resisting coatings. The Ferrotic derives its wear resistance from the TiC, while in Metco 34FP, WC particles serve the same purpose. Metco 16C and Glidden 72 are self fluxing alloys in which hard borides and silicides resist wear. The final coating contains MoS_2 as a solid state lubricant.

One additional plasma sprayed material has been prepared to explore the feasibility of producing a new type of hardened surface. A coating of titanium about 0.012 inches thick was sprayed onto 4340 tool steel with the objective of laser melting to alloy the Ti into the surface. The Ti should reduce the other carbides present to produce TiC, perhaps the most wear resistant of carbides. Of course, optimization of properties would require a higher initial carbon concentration than the 0.42 percent typically present in 4340, but experiments on this material should reveal the effectiveness of the reaction.

Table II lists three corrosion resisting coatings which were prepared by plasma spraying. Additionally, some of the materials listed in Table I have good corrosion resisting properties when properly processed. The stainless steel coating listed in Table II is a standard alloy for aqueous corrosion resistance whose properties might be improved by laser melting, while the others are materials combinations which might prove attractive for energy conversion applications. Hastelloy, which has good resistance to hot corrosion, would permit energy efficient use of copper in heat exchangers if it can be consolidated by laser melting. The Ti-B coating will be fused with a view toward producing titanium borides, compounds which are widely studied because of their ability to improve the corrosion-erosion behavior of Ti in turbines.

The remaining, and perhaps most exciting, approach toward corrosion prevention which is being pursued is that of producing amorphous surface layers on crystalline materials. Two materials of promise have been plasma sprayed and others will be prepared this year. In addition, a group of electroless nickel-phosphorus coatings were deposited on Ni substrates. Because these coatings are amorphous as

deposited, they will permit a study of the resolidification behavior of a partially melted amorphous material. Melting through to the substrate will provide a crystalline solid-melt inteface for comparative studies.

The plasma sprayed materials prepared for this study are $Cu_{60}Zr_{40}$, a material which has been plasma sprayed previously to form an amorphous structure (4,5), and AWS 4777, a brazing alloy which is commercially available in amorphous strip. Coincidentally, certain of the wear resisting alloys are similar in composition to AWS 4777 and may prove of interest in this effort. For example, the X-ray studies to be discussed in the next section have shown that three of the alloys listed in Table I are partially amorphous in the as sprayed condition.

In addition to the materials discussed so far, we have contracted with APS Materials to have a series of coatings plasma sprayed in vacuum. These coatings will duplicate some of those already available such as Ti on tool steel, Ferrotic CM on tool steel, Ti-66%B on Ti, and $Cu_{60}Zr_{40}$ on Cu. These vacuum sprayed materials will allow us to test such materials variables as the effects of trapped gases, and the importance of oxides formed during spraying.

Materials Characterization

The principle means of materials characterization used to date are optical microscopy and X-ray diffraction. After irradiation these techniques will be supplemented, when appropriate, with electron microscopy, bend testing, corrosion testing, and wear testing. The latter techniques will be applied when X-ray analysis and optical microscopy suggest that the more time consuming testing is justified.

As an example of the type of information provided by the otpical microscopy and X-ray analysis employed already, we have determined that the 316L stainless steel coatings and the $Cu_{60}Zr_{40}$ coatings have an appreciable volume fraction of oxides. These oxides will likely prevent good wetting during laser melting, so with these coatings vacuum spraying may be required. More promising results were obtained on some coatings such as the Ti on 4340, which shows little evidence of oxidation.

X-ray characterization of the coatings which will be used in our attempt to generate amorphous coatings is also encouraging. Figure 6 shows X-ray traces of AWS 4777 in

three different forms. The upper trace shows the diffraction pattern of the powder as received from the vendor. The many peaks in the trace show that several crystalline phases are present. The bottom trace was obtained from an amorphous strip of the material obtained from Allied Chemical. The two broad peaks (one of low intensity) are those expected from an amorphous material. The center trace was made from the plasma sprayed coating done for us by APS Materials. The two broad maxima show that the coating is partially amorphous. The sharp diffraction peaks are from a Ni rich fcc terminal solid solution. We are optimistic that laser melting will produce a fully amorphous surface on this material. Other materials which exhibit a partially amorphous structure are the Metco 34FP, the Metco 16C, the Glidden 72, and the $Cu_{60}Zr_{40}$. However, none of these exhibit as few crystalline peaks as the 4777.

SECTION IV
INSTRUMENTATION AND MECHANISM DEVELOPMENT

Basic facilities available for laser processing include NRL's 25kW, CW CO_2 laser which can produce beams in several different configurations, and an evacuable laser processing chamber with water cooled internal moving mechanisms for laser spraying. To carry out the objectives of this program, it has been necessary to develop several devices for handling materials and for analysis of powder kinetics. Some of these systems are described in this section.

Powder Feed Devices

Efficient application of powder to a substrate surface requires that the powder be injected into the center of the high energy laser beam. We have demonstrated two methods for accomplishing this. The first method uses a water-cooled nozzle such as that shown in Figure 7. Nozzles such as this were constructed from 2.5mm o.d. thin-walled copper tubing, gold plated to enhance reflectivity and to prevent discoloration. The U shaped water cooling section shadows the powder feed section from the laser beam, and the total obstruction of the beam is only a strip 2.5mm wide running from one side into the center of the beam. This nozzle was found to survive in beams of at least $4kW/cm^2$.

The second powder injection method uses a mirror with a small hole drilled directly through its center. Powder is blown out through this hole in the direction of the beam,

which is reflected at an angle off the mirror, with sufficient velocity to move the powder past the incident beam before it is heated enough to be propelled. With a hole having a diameter of 0.5mm the power entering the hole in the mirror in a beam of density 1kw/cm^2 is only 2W, and it was found that the mirror was not damaged.

The powder is fed to the nozzle or mirror by a stream of gas regulated by a flow control system. This system is intended to bring the powder to the nozzle with a minimum volume of gas flow, particularly when spraying into a vacuum system. It was found that the gas flow needed to transport powder when spraying into atmospheric pressure was 3-5 cfh and when spraying into an evacuated chamber was 1.5cfh. With this small flow rate, it will be possible to maintain a continuous low pressure in the processing chamber. Powder particles emerged from the nozzle with velocities of typically 0.5m/sec when spraying into atmospheric pressure and 3m/sec when spraying into vacuum.

Powder is fed into the gas stream by the system shown in Figure 8. The system is constructed to allow relatively rapid changing of the powder charge, while being able to retain vacuum conditions. Powder from the reservoir is dropped into the gas stream through a sieve and shaker mechanism. Sieves are interchangeable to allow use of different powder sizes. Powder feed rate is regulated by sieve diameter and vibrator amplitude, with minimum feed rates being used for measurements of powder particle dynamics and larger feed rates for application of coatings.

Pyrometry and Particle Velocity

The temperature histories of laser heated powder particles cannot be measured by standard pyrometric methods. Though the radiant intensity of each particle is high, the small particle size and short interaction time require high sensitivity and speed of the radiometric device employed. This dual requirement necessitates the design of a special pyrometry system.

We investigated photographic methods whereby an image would be alternately attenuated by color filters. Densitometric measurements of the exposed film images would yield wavelength ratios which could be calibrated for temperature. It was found that if the system is to be used with temperatures of 1000°C or lower, the film exosures of the filtered images were impractically low even when broadband color filters were used.

Since the total radiation from a particle varies as

T^4, a photographic measurement based on total (unfiltered) image density was considered. The calibration of such a system would require a consistent photographic and optical procedure from film acquisition to processing. This consistency requirement was considered achieveable but difficult. An analysis of optical resolution and field of view effects on film exposure revealed that photographic images would depend on particle size and position in the field of view direction. Since these effects could not be corrected accurately, total radiation methods were ruled out.

The idea of a totally imaged dynamic temperature measurement was discarded in favor of viewing a small, selectable area for each laser irradiation. The area can be chosen so that particles are viewed individually or as a collection. The light can be split and/or filtered to be measured by photomultiplier tubes which have the speed and sensitivity required.

A block diagram of the constructed system is shown in Figure 9. A high efficiency collector lens and focusing lens image the object radiation onto a flat plate with selectable central aperture. Here, the region in the object plane is chosen as well as the viewing area. The apertured radiation is then collimated and divided by a diferential beam splitter. The splitter reflects wavelengths greater than 0.6μm and transmits shorter values. The two collimated beams are then focused onto separate photomultiplier detectors. The detectors are operated in high gain and pulsed for $\sim$ 75 ms duration.

Note that with this system, both signals are monitored simultaneously (no chopping) without throwing away significant amounts of light to get wavelength discrimination. Thus, the speed and sensitivity requirements have been met at the expense of image resolution. A prelimnary calibration of the system yielded ratios of the "red" to "blue" signals that varied by an order of magnitude for temperatures of 1000-3000°K.

The system was tested for sensitivity by dropping alumina powder into a hydrogen flame. The resulting data is shown in Fig. 10 with the upper trace representing the "red" channel. Individual particles can be observed and correlated between channels. Single particle transit times of 1ms yield velocities of 2-10 m/s which is similar to the laser spray data obtained so far. Torch operation at low flow rates resulted in broader data peaks with a high red ratio indicating slower, cooler powders.

We are in the process of procuring an optical spectrometer which also views small areas of the object plane. A multi-element detector array gives more spectral resolution than our 2 channel system described above. The spectrometer can be operated in a mode whereby very short scan times are employed, or a time integrated signal can be obtained. The sensitivity will allow the monitoring of a small number of particles (3-6) or a region of many particles. The added spectral resolution will be valuable in determining average powder temperatures and the presence of vapor species.

Particle velocities are measured by forming a photographic image of the incandescent particles, with a mechanical light chopper in the optical train. The system is shown in Figure 11.

Surface Melting

A surface melting apparatus has been designed and built which combines rapid setup and ease of operation with wide flexibility in processing capability. The apparatus was designed to permit either single pass or multiple pass melting. With single pass melting the beam power and sample translation speed can be varied systematically to quickly determine on a small sample the optimum processing conditions. Using these conditions, and employing a unique specimen translation mchanism, the apparatus permits uniform glazing of specimens as large as 2.5 x 6 inches.

The apparatus is easily moved by two people and can be set in the laser laboratory without disrupting other experiments. Thus it is possible to set up quickly and acquire data on a shorter time scale than is required for more cumbersome equipment. It consists of a two foot diameter aluminum table which is spun by a variable speed electric motor, and upon which are mounted sample holders which incrementally translate the specimens between passes under the laser beam.

The incremental sample translations, which are accomplished by a gear device that is advanced with each table revolution, can be as little as 0.2 mm or as much as 1.2 mm, a range which spans the breadth of expected individual melt passes. The specimens are protected from oxidation by an inert gas shield.

SECTION V
POWDER KINETICS MEASUREMENTS

A series of experiments has been carried out to

determine the kinetics of particles in laser beams as a function of particle size and power density. In these experiments we used a beam of top-hat geometry reflected off a concave mirror such that the beam diameter decreased from 3.8cm at the mirror to a focal point 110cm from the mirror. Powder was injected into the beam by means of a nozzle located at the point where the beam diameter was 1.9cm, and powder velocities and temperatures were measured 15cm downstream from the nozzle, where the beam diameter had decreased to 1.3cm. The total beam power was varied between 2 and 10kW (resulting in power densities at the point of measurement ranging from 1.5 to 7.5kW/cm^2) and three different sizes of sorted aluminum oxide powders were used; -230+325 mesh (45-63μm diameter), -170+200 mesh (75-90μm diameter), and -100+140 mesh (106-150μm diameter). Velocities of numerous particles were measured for each particle size and laser beam power. Normalized histograms resulting from these measurements are shown in Figures 12, 13, and 14.

As expected, the velocity histograms show considerable scatter. Much of this can be attributed to particles which are travelling along the periphery of the laser beam, or which have passed out of the beam but are still glowing. Because most photographs showed overlapping tracks or tracks which were faint or out of focus, it was necessary to be selective in choosing tracks for measurement. Emphasis was directed toward the faster tracks in each photograph, because these represent particles which have remained within the uniform region of the laser beam. However, bright clear tracks lying within the central region of the photograph were also measured, even if they were clearly travelling well below the maximum velocity. The histograms reflect these selection choices in that they do not include the tracks of faint, slow moving particles.

The overall trend of the histograms with increasing beam power is evident. The velocities are not great because the measurements were carried out in a wide part of the beam so that the power density would be reasonably uniform. Two other presentations of the same data are shown in Figures 15 and 16. Figure 15 shows the average measured particle velocity at each power density and particle size, while Figure 16 shows the average of the four fastest particles measured under each set of conditions. The latter is thought to be more representative of particles which have remained within the beam. Again the variation of velocity with power density is clear and the trend is as expected.

The variation of velocity with particle size, however, is more surprising in that it shows a definite maximum for the intermediate size prticles. The relatively slow velocity of the smallest particles is undoubtedly attributable to atmospheric drag. Qualitatively, it was observed that the smallest particles were the most strongly affected by convective air currents. Under vacuum conditions, the particles should not attain steady-state velocities, and the smaller particles should accelerate most rapidly.

Because many particles were swept out of the laser beam by the convective air currents, a quartz tube with a diameter of 2.5cm and a length of 30cm was placed around the laser beam immediately downstream from the nozzle. This was extremely effective at keeping the powder within the laser beam with the result that a large fraction of the powder was accelerated to near the maximum velocity. Further experiments with this type of device are contemplated.

SECTION VI
STATUS OF THE PROGRAM

The initial stages of the program emphasized materials acquisition and the design of systems for materials processing and analysis, while actual use of the NRL laser was delayed until it became available in October, 1978. Since that time, work has progressed rapidly on both laser spraying and surface melting aspects of the program. In addition to the particle velocity measurements described in this report, particle temperatures were successfully measured with the pyrometry system. Preliminary analysis of the data indicates that the masured temperatures agree with calculated values in the vicinity of the melting point, but that at higher power densities the particles are cooler than predicted. The processing table has been used to surface melt a large number of plasma sprayed coatings and other materials, and to carry out uniform melting on the surface of a 2 X 6 inch test sample. The surface melted samples are now being analyzed.

The laser processing chamber, manufactured by AVS in Ayer, Mass., has now been delivered after long delays caused by difficulties with rotating water-cooled seals. The chamber is now undergoing modifications to incorporate design improvements, and to increase its mobility so it can be moved in and out of the cramped quarters of the laser test cell.

No significant difficulties are anticipated in carrying out the laser processing tasks of this program. The facilities available are capable of producing test samples at a rapid rate, such that the subsequent sample evaluation is the rate-limiting step.

REFERENCES

1. K. Yamamoto and M. E. H. VanDongen, J. Colloid and Interface Science, 57, 162-165 (1976).

2. Yu. I. Yalamov, V. B. Kulukov, and E. R. Shchukin, J. Colloid and Interface Science 53, 564-571 (1976).

3. H. S. Ingham, Jr. U. S. Patent 3,310,423, March 21, 1967.

4. H. S. Chen and C. E. Miller, Rev. Sci. Instr., 41, 1273 (1970).

5. B. C. Giessen, N. M. Madhara, R. J. Murphy, R. Ray and J. Surette, Met. Trans. A, 8A, 364 (1977).

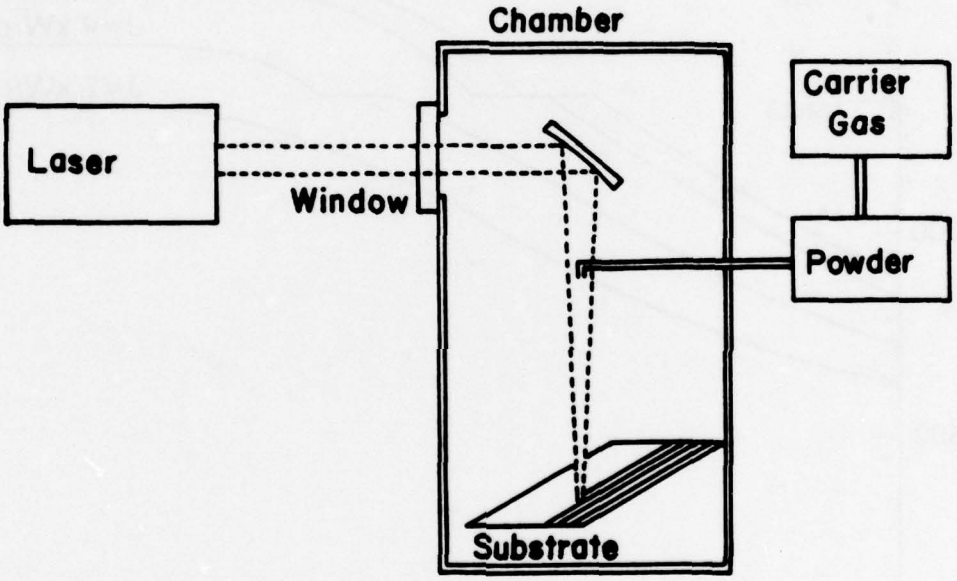

Fig. 1 — The laser spraying process

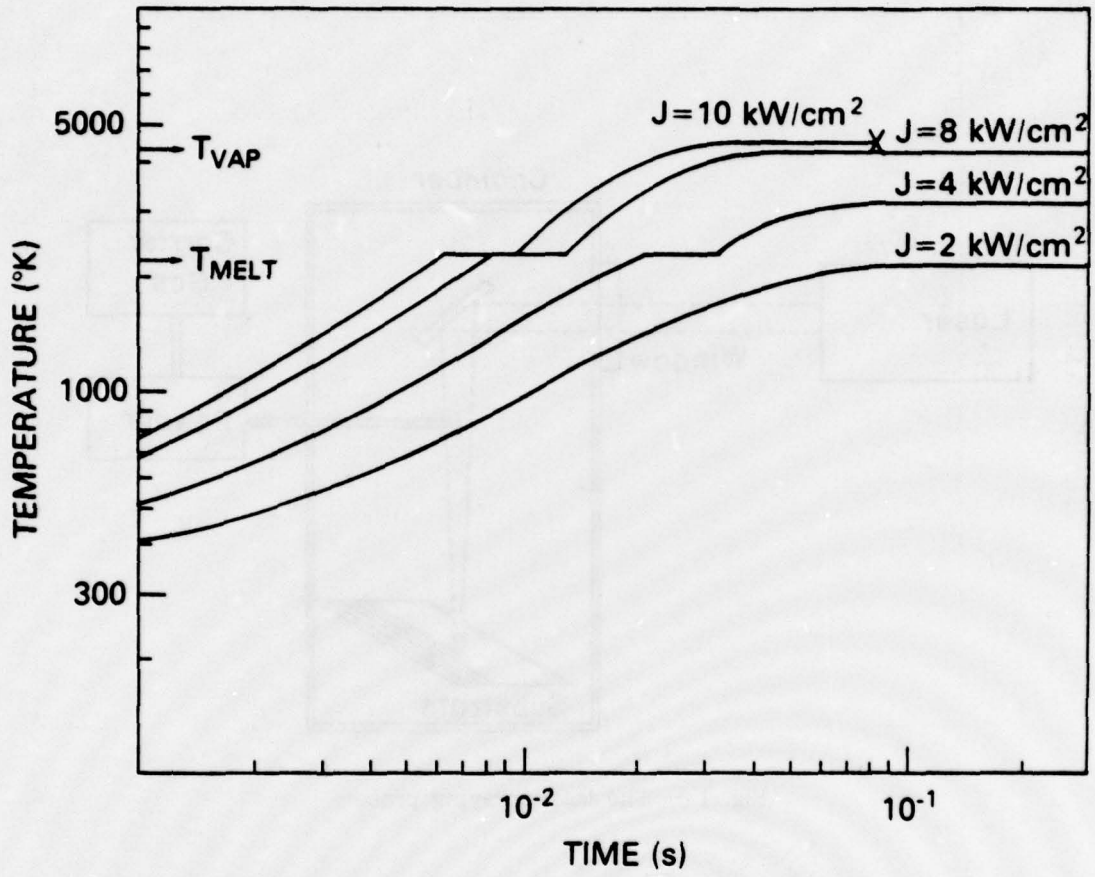

Fig. 2 — Temperature profiles for an Al_2O_3 particle irradiated by a 10.6 μm laser flux in air. Laser wavelength = 10.6 μm; particle radius = 40 μm.

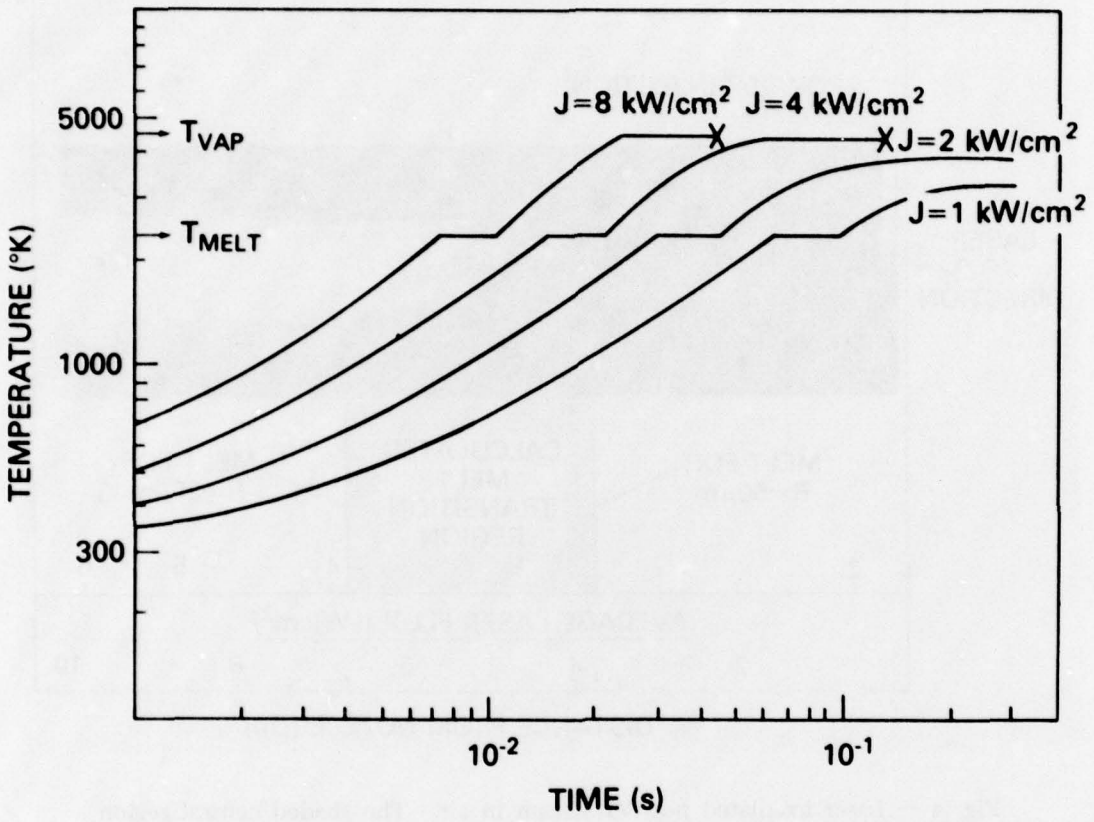

Fig. 3 — Temperature profiles for the same particle irradiated in vacuum

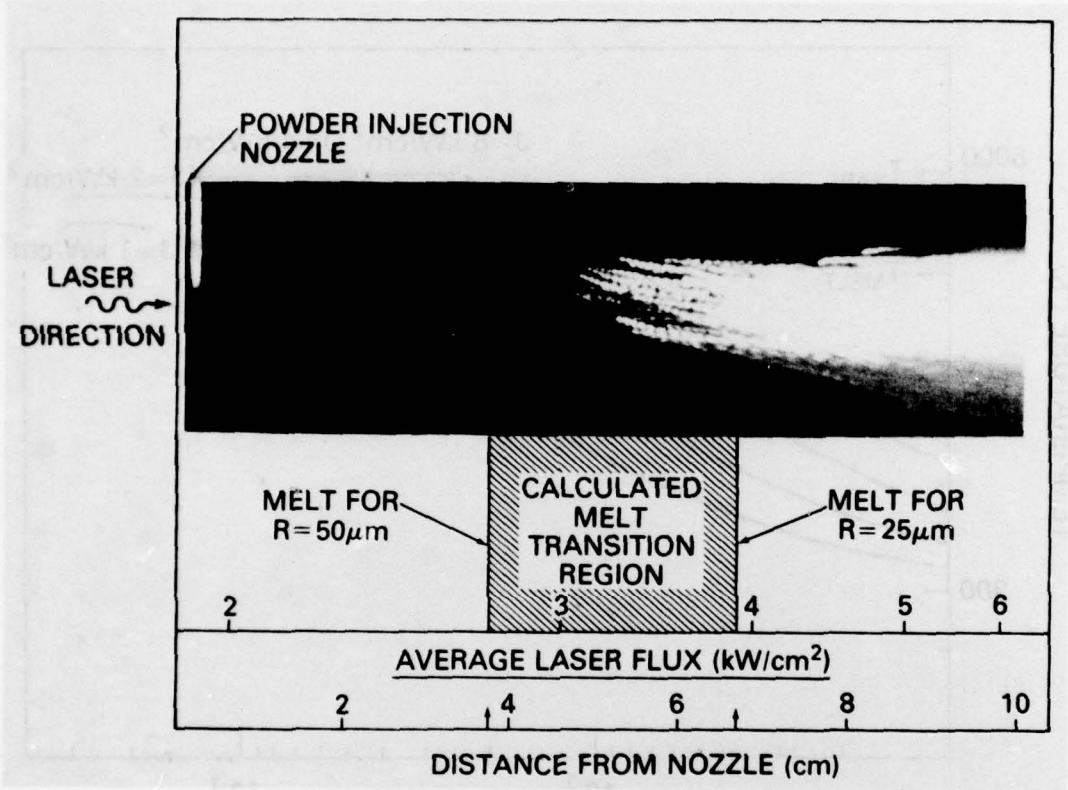

Fig. 4 — Laser irradiated powder stream in air. The shaded central region predicts positions where particle melting should be reached depending on initial powder size.

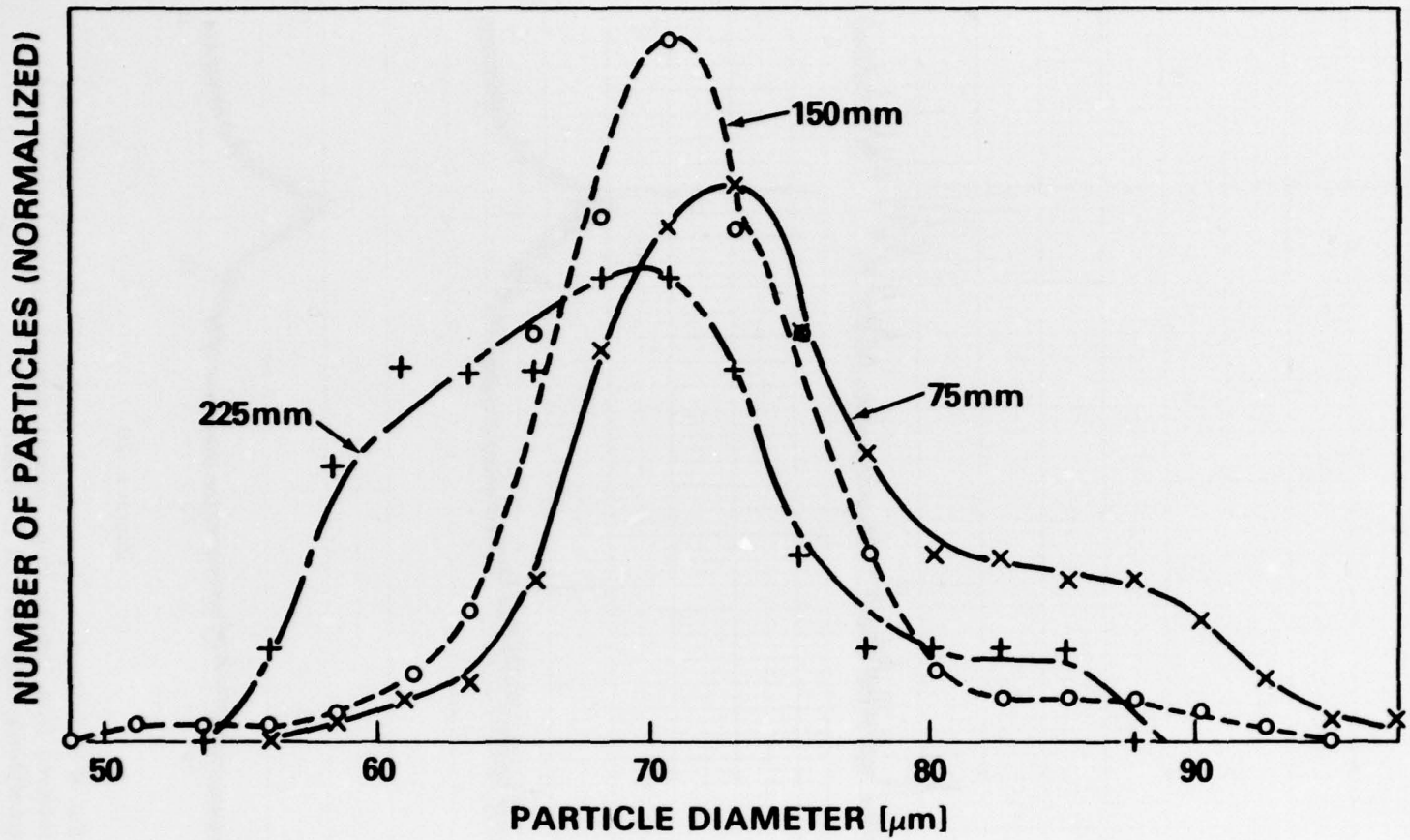

Fig. 5 — Diameters of aluminum oxide particles after transport for 3 different distances in a 6 kW laser beam

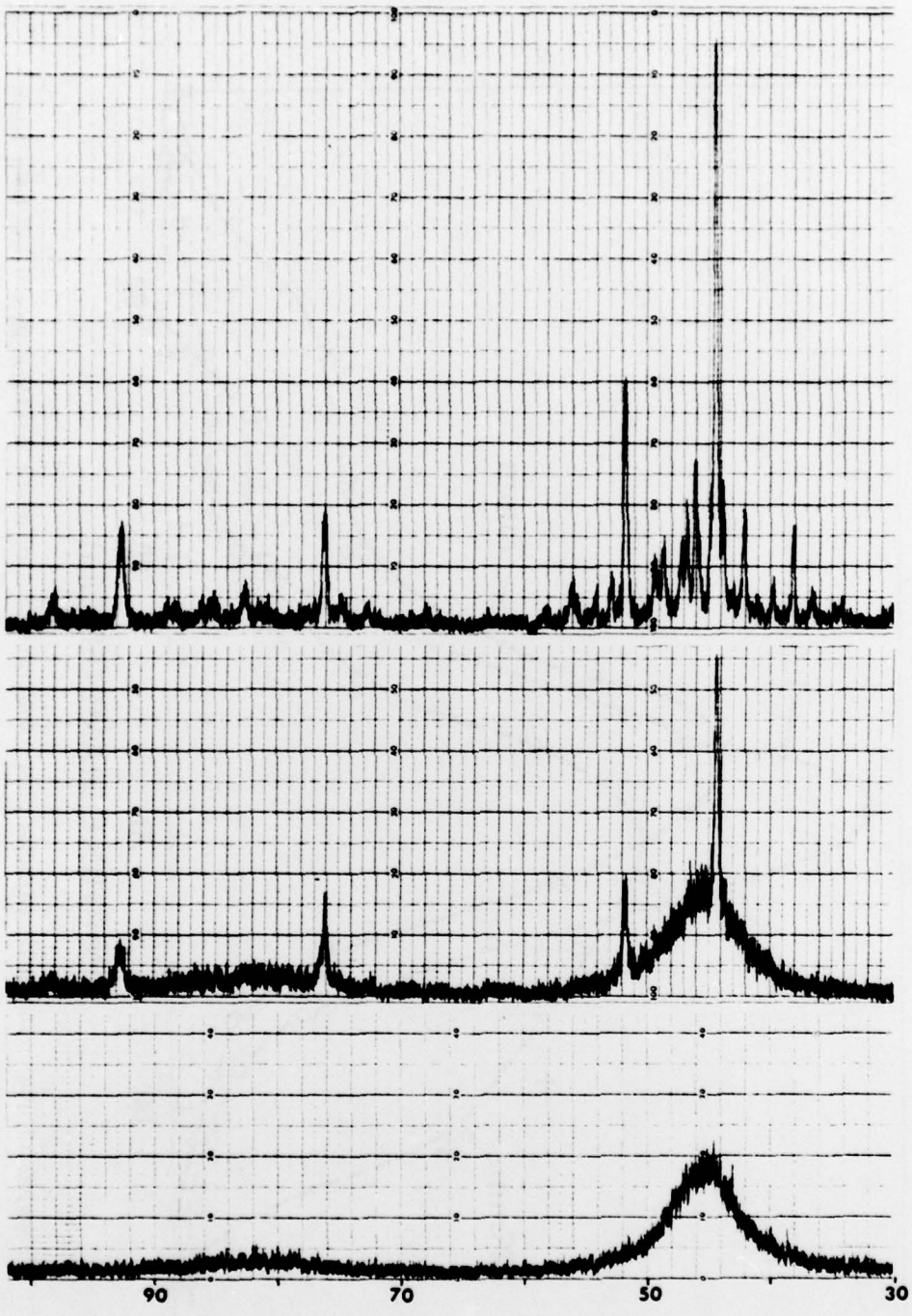

Fig. 6 — Diffractometer scans of AMS 4777 in form of powder received from vendor (top), plasma sprayed coating (center) and amorphous strip material (bottom)

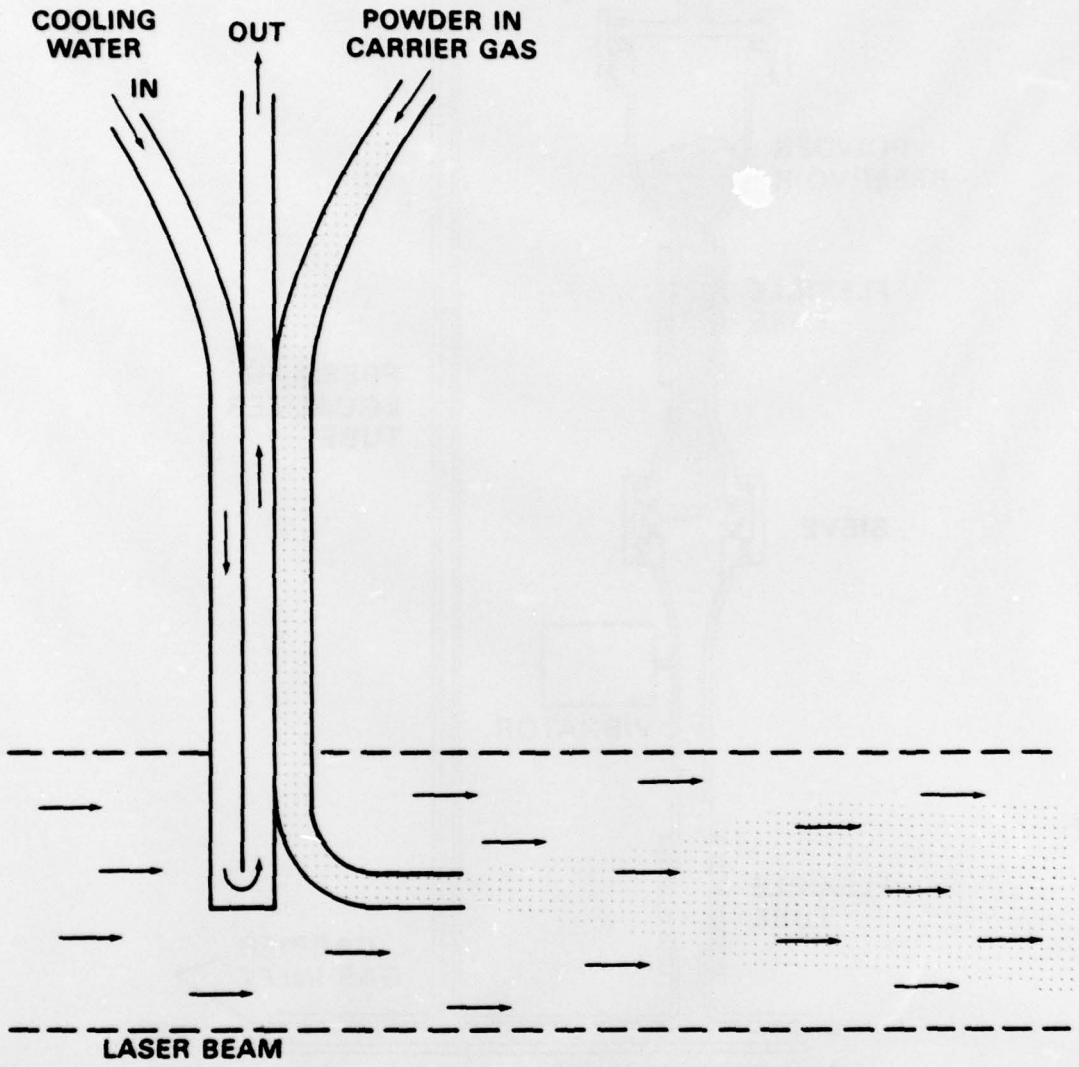

Fig. 7 — Water cooled nozzle for injection of powder into high energy density laser beam

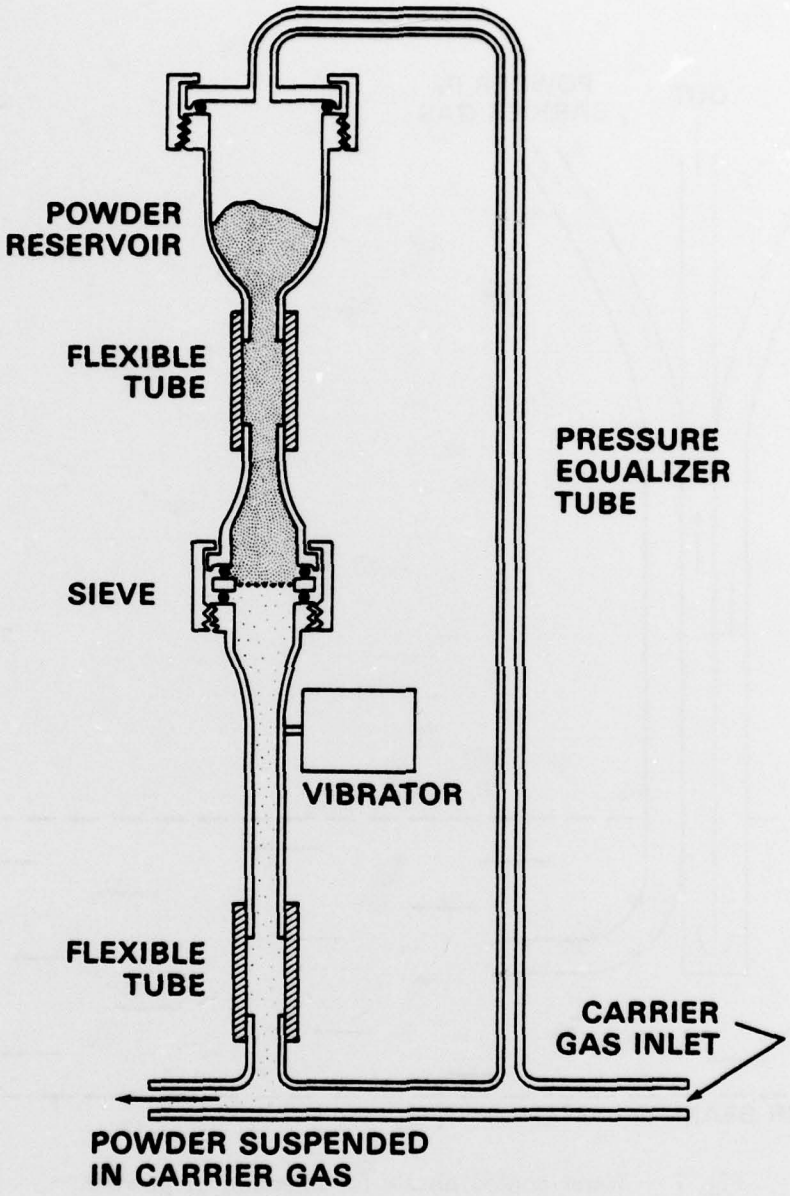

Fig. 8 — System for feeding powder into vacuum system

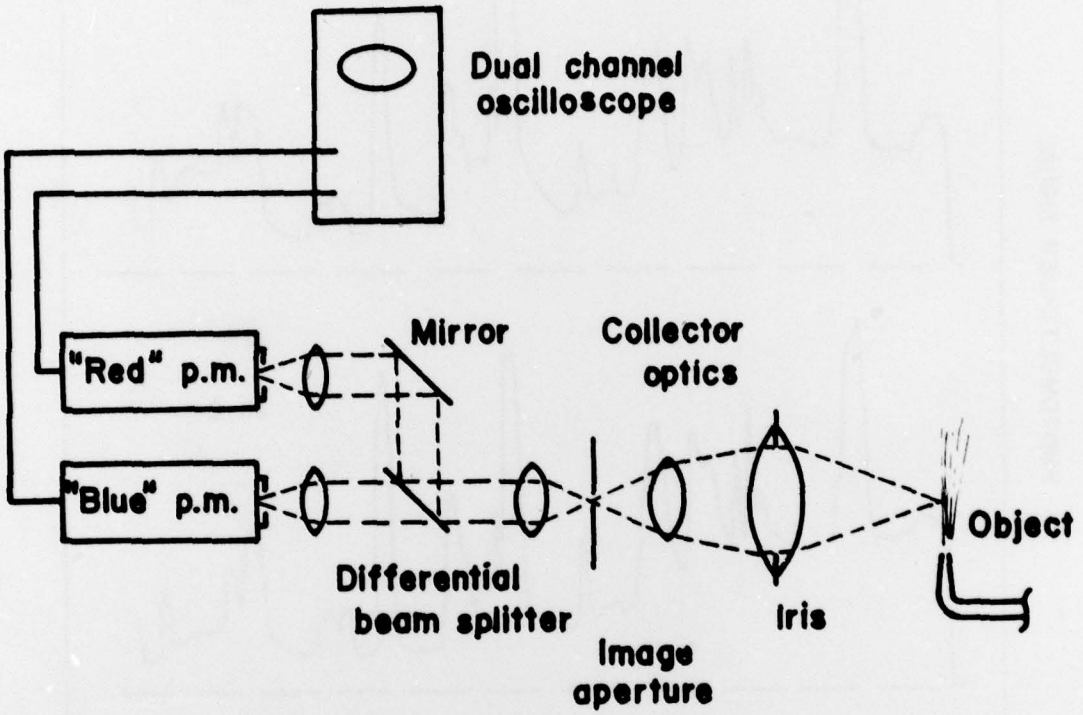

Fig. 9 — Schematic diagram of the NRL transient pyrometry system developed for laser-irradiated powder detection

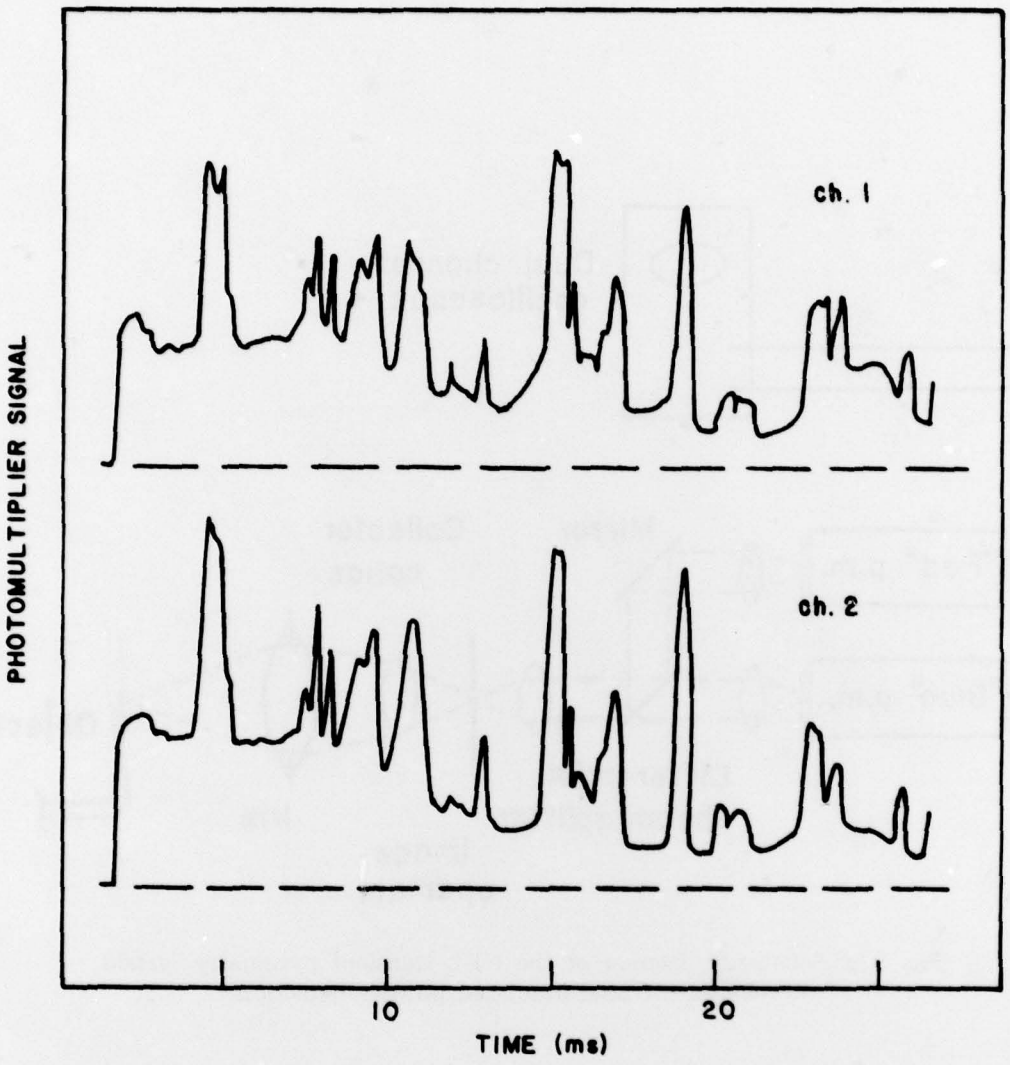

Fig. 10 — Pyrometer response to Al_2O_3 particles heated by an H_2-O_2 torch in air. The upper channel has a peak wavelength response at 0.7 μm ("red"); the lower channel peak is at about 0.5 μm ("blue").

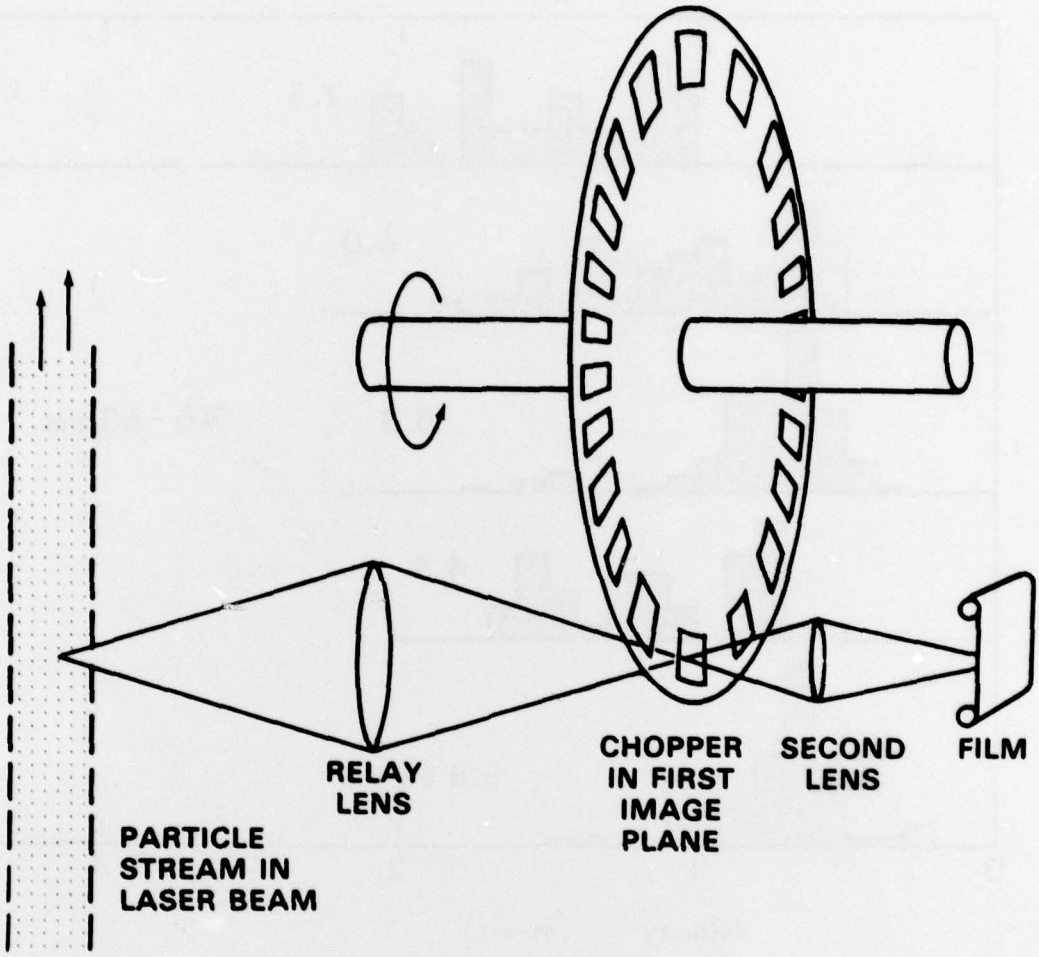

Fig. 11 — Photographic system for particle velocity measurement. The image is mechanically chopped at 1 kHz.

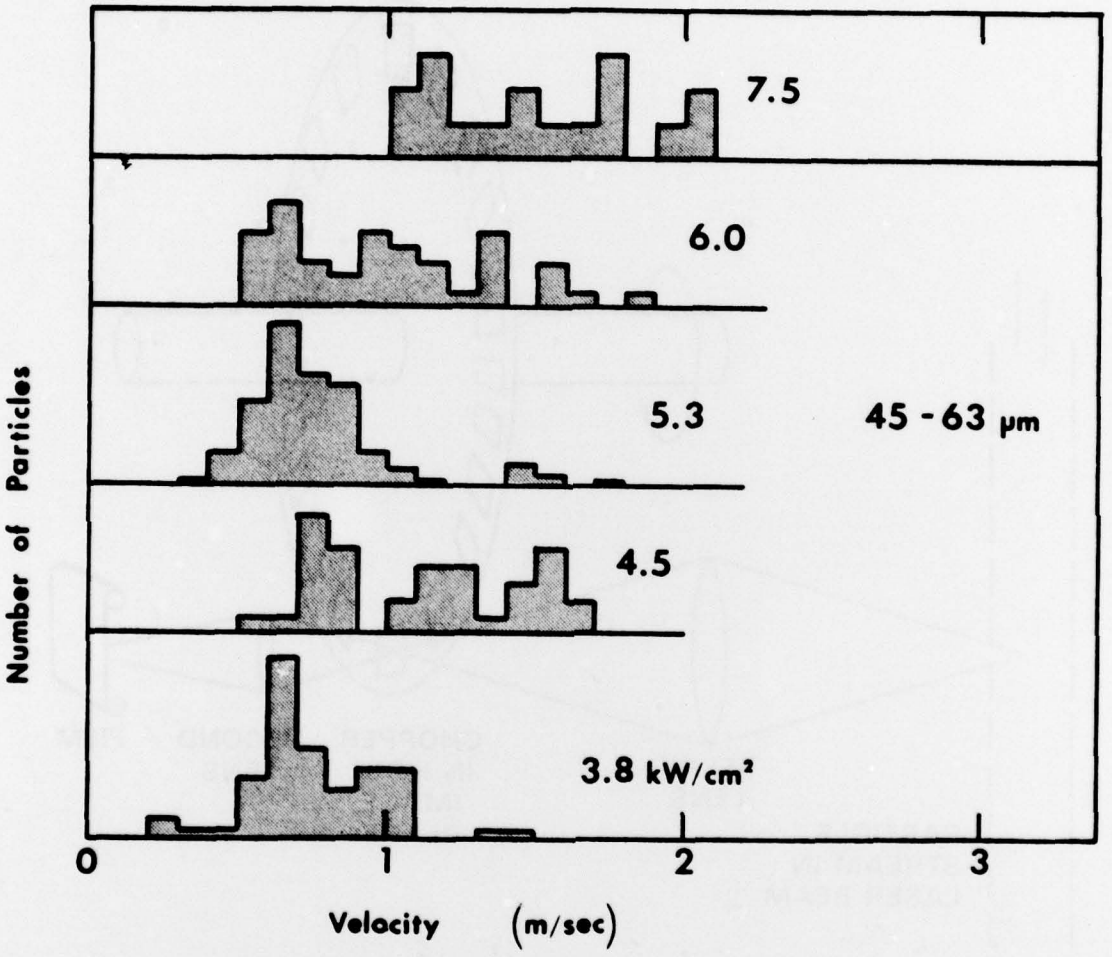

Fig. 12 — Normalized histograms of particle velocities at different laser power densities, for Al_2O_3 particles with diameters of 45-63 μm

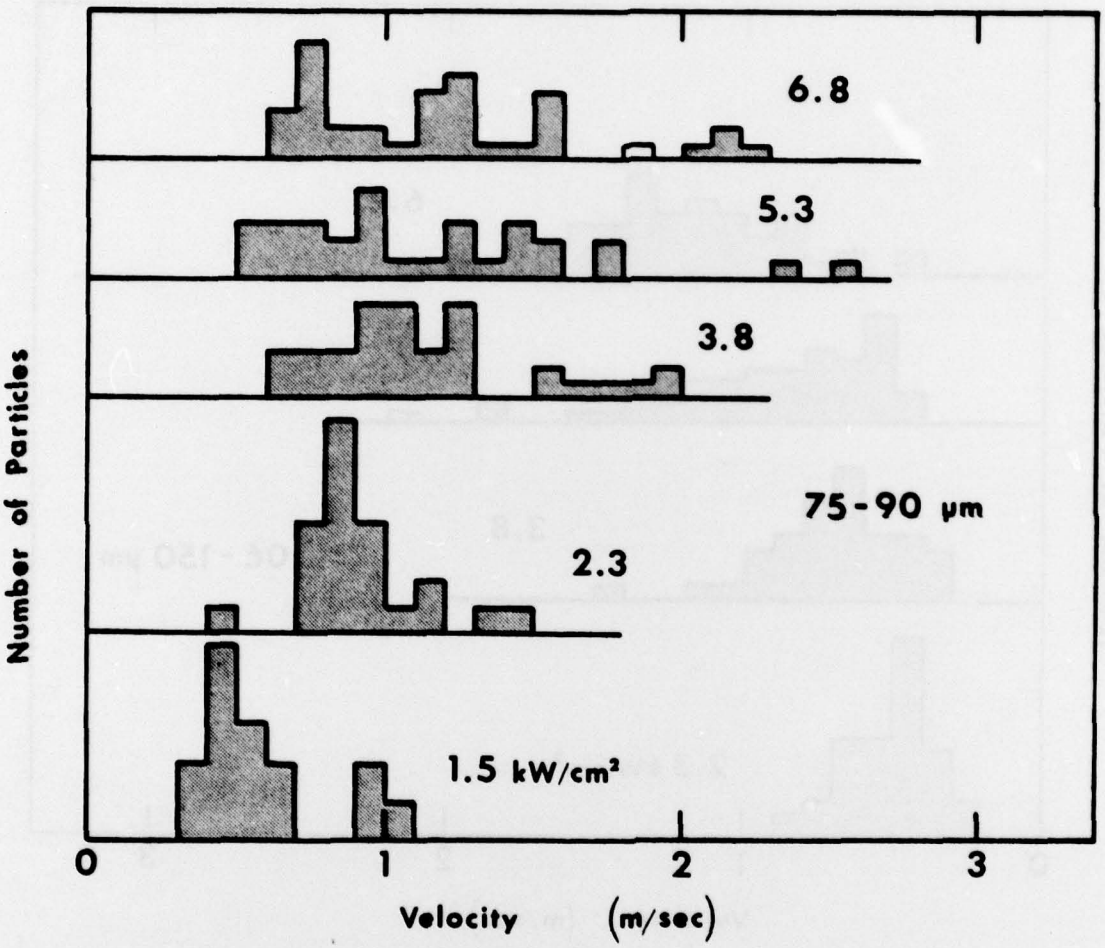

Fig. 13 — Normalized histograms of particle velocities at different laser power densities, for Al_2O_3 particles with diameters of 75-90 μm

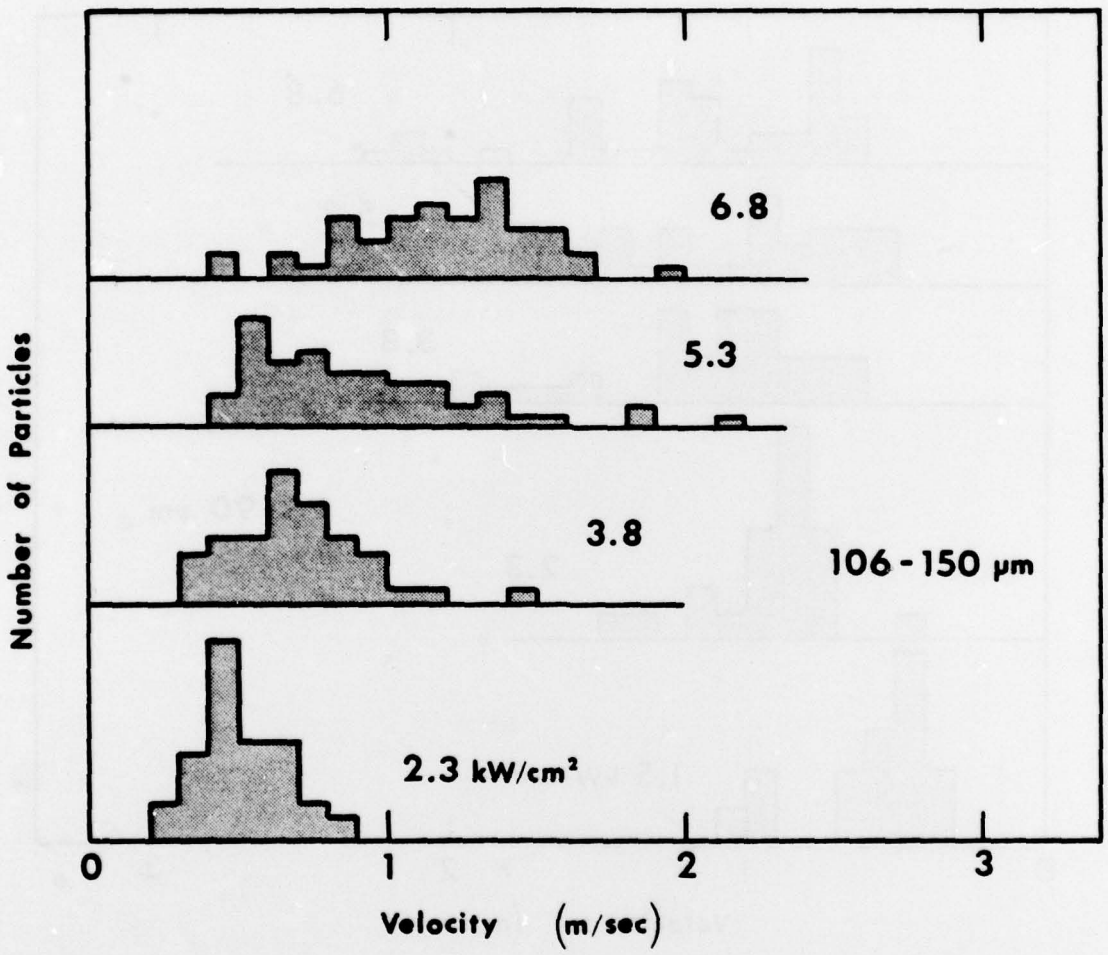

Fig. 14 — Normalized histograms of particle velocities at different laser power densities, for Al_2O_3 particles with diameters of 106-150 μm

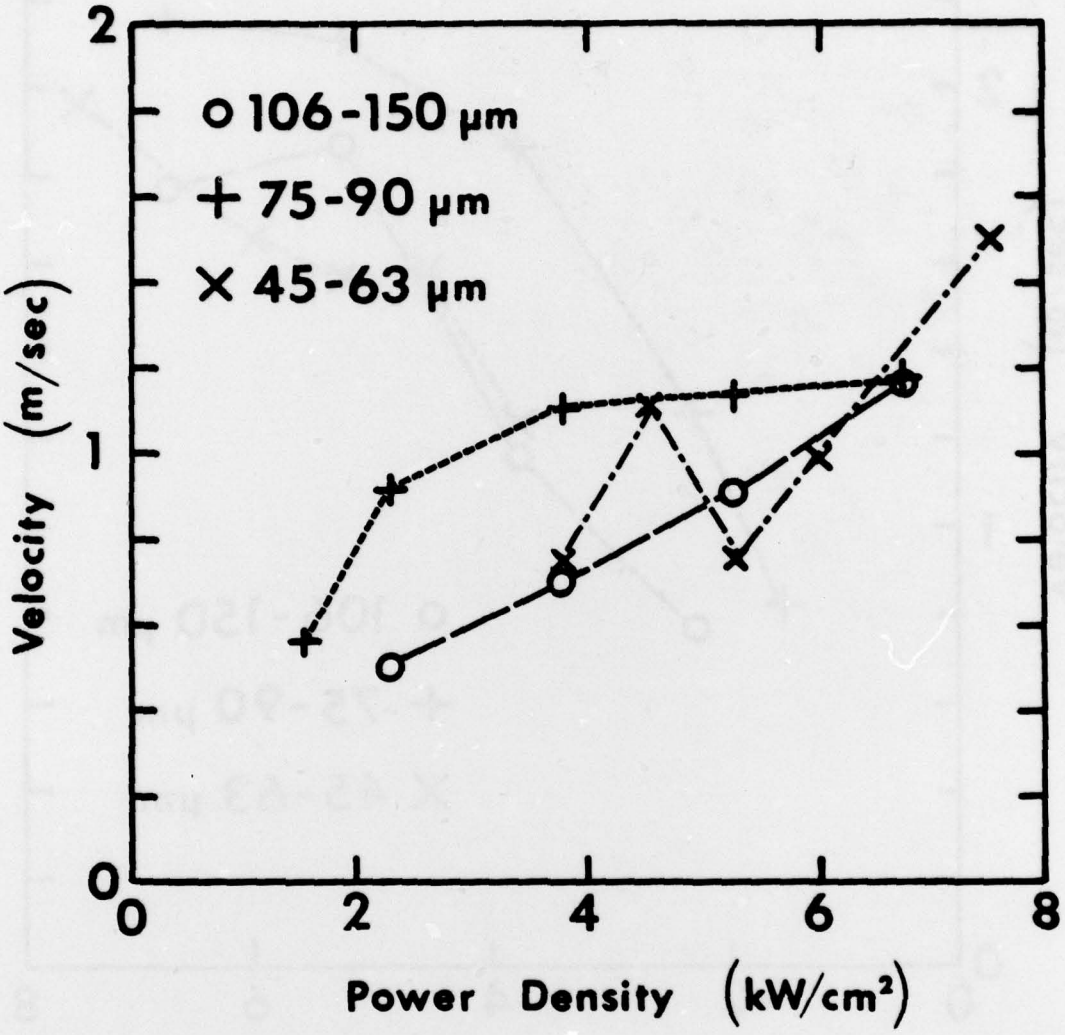

Fig. 15 — Average measured particle velocity, as a function of laser power density, for three different size of Al_2O_3 powder

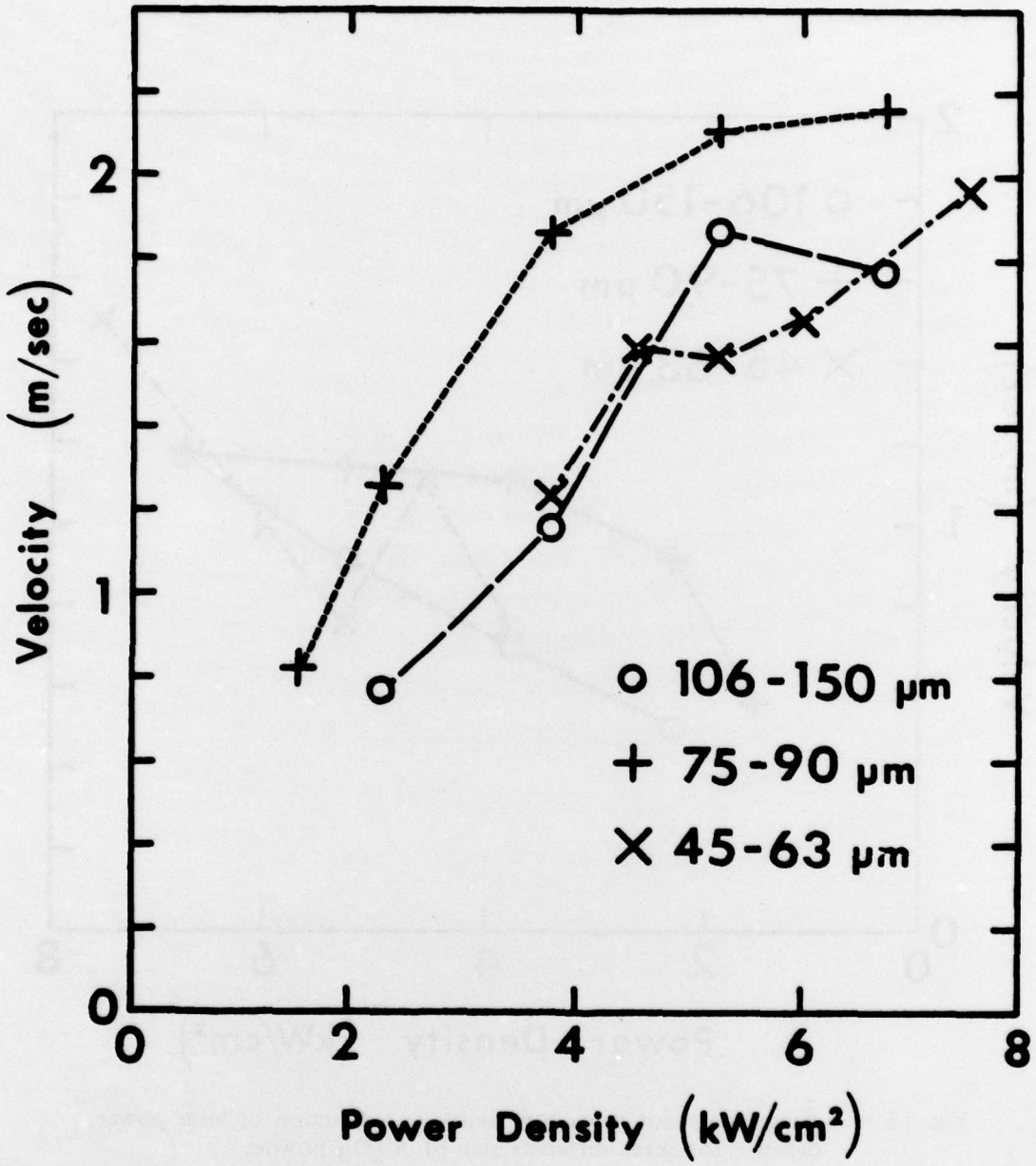

Fig. 16 — Average of the four fastest measured particles, as a function of power density, for three different sizes of Al_2O_3 powder

TABLE 1
PLASMA SPRAYED WEAR RESISTING COATINGS

COATING MATERIAL	SUBSTRATE	COATING THICKNESS (10^{-3}in)
FERROTIC CM	4340 STEEL	12-15
METCO 34FP	4340 STEEL	12-15
METCO 16C	LOW CARBON STEEL	21-23
GLIDDEN 72	LOW CARBON STEEL	12-24
HARDFACEING ALLOY WITH 10 wt% MoS_2	LOW CARBON STEEL	21-23

TABLE II
PLASMA SPRAYED CORROSION RESISTING COATINGS

COATING MATERIAL	SUBSTRATE	COATING THICKNESS (10^{-3}in)
316L STAINLESS STEEL	LOW CARBON STEEL	5 and 21-23
HASTELLOY C	COPPER	16
Ti-66%B	Ti	20